28 Oct 2022

Further Comments on "Engineering Shape Anisotropy of Fe3o4-Γ-Fe2o3hollow Nanoparticles for Magnetic Hyperthermia"

Fernande Grandjean
Missouri University of Science and Technology, grandjeanf@mst.edu

Gary J. Long
Missouri University of Science and Technology, glong@mst.edu

ACS APPLIED NANO MATERIALS

www.acsanm.org

Comment

Further Comments on "Engineering Shape Anisotropy of Fe_3O_4-γ-Fe_2O_3 Hollow Nanoparticles for Magnetic Hyperthermia"

Fernande Grandjean* and Gary J. Long*

Cite This: *ACS Appl. Nano Mater.* 2022, 5, 14031−14037

Read Online

ACCESS | Metrics & More | Article Recommendations | Supporting Information

ABSTRACT: In their earlier paper, Niraula et al. (*ACS Appl. Nano Mater.* **2021**, *4*, 3148−3158) described the morphological, compositional, and magnetic properties of three different magnetite/maghemite or Fe_3O_4/γ-Fe_2O_3, hollow nanoparticles, referred to herein as nanorings, short-nanotubes, and long-nanotubes. Scanning electron microscopy indicates that these nanoparticles have lengths of 275 ± 51, 411 ± 92, and 515 ± 98 nm and outer diameters of 201 ± 55, 251 ± 46, and 229 ± 42 nm, respectively, dimensions that are all rather similar in view of their distributions, as is shown in a figure herein. Further, the lengths indicate that these nanoparticles are far larger than what are normally considered nanoparticles. Rietveld refinement of the powder X-ray diffraction patterns presumably reveals the presence of Fe_3O_4, γ-Fe_2O_3, and small amounts of α-Fe_2O_3 in some of the nanoparticles; unfortunately, the lack of refinement details make the validity of these compositions at least problematic. The published iron-57 Mössbauer spectral analysis is marginal. An alternative analysis of both the reported X-ray lattice parameters and the Mössbauer spectral results for the three nanoparticles in terms of solid solutions of magnetite and maghemite, $^{A}Fe^{3+}[^{B}Fe_{1-3\delta}{}^{2+}Fe_{1+2\delta}{}^{3+}\square_{\delta}]O_4$, where $\square$ represents a vacancy, $\delta = 0$ corresponds to magnetite, Fe_3O_4, and $\delta = 0.333$ corresponds to maghemite, γ-Fe_2O_3, is proposed herein. In the presence of the expected magnetite Verwey transition, the Mössbauer spectral analysis is formulated with the stoichiometry $^{A}Fe^{3+}[^{B}Fe_{2(1-3\delta)}{}^{2.5+}Fe_{5\delta}{}^{3+}\square_{\delta}]O_4$, and as far as we can tell, this model is consistent with the Rietveld X-ray diffraction analysis. The values of $\delta = 0.28(2)$ and $0.30(1)$ obtained from the X-ray diffraction and Mössbauer spectral analyses, respectively, indicate that the composition of the nanoparticles is very close to γ-Fe_2O_3, in contrast to the earlier conclusion. During the course of this reformulation, numerous errors in the mathematical expressions, and in some cases their subsequent misuse, have been discovered and corrected herein whenever possible.

KEYWORDS: *magnetite and maghemite solid solutions, Mössbauer spectroscopy, magnetic shape anisotropy, X-ray diffraction*

INTRODUCTION

The title of the paper by Niraula et al.[1] under consideration herein promises, first, "engineering shape anisotropy" of new materials that, second, may yield "nanoparticles for magnetic hyperthermia" applications. Both of these "promised" topics are of interest to the readers of *ACS Applied Nano Materials*. Unfortunately, the authors largely fail to deliver on these promises.

The scanning electron microscopy images (Figures 2 and S10 in ref 1) reveal that the resulting nanorings and both the short- and long-nanotubes all have, to a first approximation, the same mean lengths and outer diameters, D_{out}. This similarity is well illustrated in Figure 1, which shows the mean distances and their corresponding distributions, as obtained by assuming a Gaussian distribution of their lengths and outer diameters, D_{out}. However, it should also be noted that, although the Gaussian fits for the parameters[1] for the nanorings and sample S are reasonable, the Gaussian fits for the short- and long-nanotubes are far from satisfactory and are, at best, a good approximation of the actual size distribution.[2] Further, it should be noted that the length dimensions of the particles under study are far larger than what are typically referred to as nanoparticles. Indeed, the mean lengths range from ca. 0.300 μm for the nanorings up to ca. 0.500 μm for the long-nanotubes; perhaps they would be better referred to as mesorings and short- and long-mesotubes.

The second promise dealing with "magnetic hyperthermia" may well be a new topic to many readers as it was to the authors of this "further comment", authors who have worked in the field of Mössbauer spectroscopy and magnetic studies for approximately 50 years each.[3] So, our interest was piqued by this portion of the title, but although we have learned a good deal from this study, we have also devoted our time to trying to understand the various mathematical models and equations, several of which are either incomplete or erroneous and involve mixed unit systems or the wrong units when used by Niraula et al.[1] These various problems are discussed in detail in the Mathematical Equation Problems section.

In their Introduction, Niraula et al.[1] present a useful discussion as to why the presence of divalent iron in magnetite, Fe_3O_4, makes it a poor candidate for magnetic hyperthermia clinical applications and use—at least in any pristine uncoated form. Unfortunately, they fail to emphasize that their phase analyses by powder X-ray diffraction and Mössbauer spectros-

Received: August 12, 2022
Accepted: September 15, 2022
Published: September 29, 2022

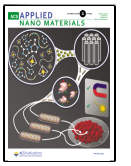

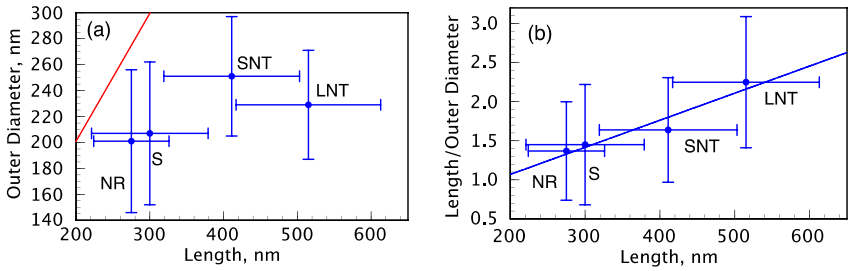

Figure 1. Mean outer diameter, D_{out}, versus mean length (a) and the ratio of the length/outer diameter, ρ, versus length (b) of the nanorings, NR, the short-nanotubes, SNT, the long-nanotubes, LNT, and sample S, as published by Niraula et al.[1] and obtained from the Gaussian distribution of the particle lengths and outer diameters, as revealed by scanning electron microscopy. In part a, the red line corresponds to the values of the outer diameters that would correspond to isotropic nanotubes. These two plots reveal the high similarity between all of the nanoparticles when their size distributions are considered. The uncertainties have been obtained from the half-width at half-height of the Gaussian distributions.

copy indicate that, in the nanorings and short- and long-nanotubes, the major phase[1] present is magnetite. However, the authors of this comment noticed that there were obvious deficiencies in the fits of the Mössbauer spectra shown in Figure 4 published by Niraula et al.[1] As a consequence, the Mössbauer spectra shown in this figure have been refit herein, and a very different analysis in terms of solid solutions of Fe_3O_4 and γ-Fe_2O_3 is presented in the Mössbauer Spectroscopy section.

Nayak[4] has already commented on the paper by Niraula et al.[1] and noted that the fit of two γ-Fe_2O_3 components in the Mössbauer spectra is unacceptable because of the problematic fit of two different iron(III) magnetic sextets, which are typically very poorly resolved, if resolved at all, with very similar hyperfine parameters. Nayak[4] has also noted that Niraula et al.[1] do not provide a percent transmission scale for the Mössbauer spectra found in their Figure 4 nor do they report the line widths of the spectral components in their reported fits. We completely agree with this criticism.

Niraula and Sharma[5] have replied to Nayak[4] that they "... still stand with our original fitted spectra, which require no further corrections". Thus, they fully stand by their published γ-Fe_2O_3 component sextets and believe that no changes are necessary. Further, they do not provide or even mention the missing percent transmission scale or the line width of the spectral components, two very important parameters that would help in allowing the reproduction of their analysis by a reader. We completely disagree with their conclusion[5] based on the new fits shown herein and discussed below.

POWDER X-RAY DIFFRACTION RESULTS

Because the analysis of the Mössbauer spectral results, to be discussed next, clearly depend on the analysis of the powder X-ray diffraction results reported by Niraula et al.,[1] it is important to evaluate the reliability of their analysis. Sadly, this is hard to do because far too little information is provided to confirm the analysis. It is virtually impossible to confirm the increase or decrease, if any, in the area of the γ-Fe_2O_3 diffraction components on the basis of the very weak (116) reflection. This reflection at $2\theta = 27.3°$ (see their Figure 3a) is said by the authors[1] to be "a very broad" reflection. γ-Fe_2O_3 is, of course, the one component that is perhaps the most important in the utility for hyperthermia treatments with the nanoparticles under study; see the Introduction of ref 1.

Also, it seems unrealistic to believe that the Rietveld refinements yield the quoted[1] uncertainties (see their Table S3) in the lattice parameters, all of which are given as ca. ±0.005 nm, a value that seems to be independent of the amount of the component present in a given sample. It is well-known that the estimated standard deviations obtained from Rietveld refinements take into account[6] only the statistical quality of the data and do not account for any fitting model inadequacy, which may well be the case in Table S3 of ref 1.

Some of the missing information that would help to confirm the Rietveld refinements include the iron(II)- or iron(III)- to oxygen distances, the refined isotropic thermal factors, the reflection line shape, the background correction procedure, and the iron(II), iron(III), and oxygen form factors. Of course, all of this information could have been included in their Supporting Information but was not and so, sadly, the reader must accept the powder X-ray diffraction refinement results as given and hope they can be confirmed by the Mössbauer spectral studies.

The lattice parameters of 0.836(5) and 0.835(5) nm, each quoted three times in Table S3,[1] for Fe_3O_4 and γ-Fe_2O_3, respectively, are both identical within their uncertainties. In view of the detailed study by Cervellino et al.[7] of the size and compositional dependence of the lattice parameter of solid solutions of Fe_3O_4 and γ-Fe_2O_3 present in nano- and microparticles, the above values fall above the range of 0.83449−0.83479(6) nm for "maghemitic" particles[7] and below the 0.8394 nm value for "magnetitic" particles. The similarity of 0.836(5) and 0.835(5) nm seems to indicate that the lattice parameter of 0.8355(10) nm is an average lattice parameter for a solid solution of Fe_3O_4 and γ-Fe_2O_3, a solid solution that is rich in γ-Fe_2O_3, because 0.8355 nm is closer to the range for "maghemitic" particles than the value for "magnetitic" particles and not rich in Fe_3O_4, as indicated in Table S3.[1] From Figure 2a in ref 7, a lattice parameter of 0.8355 nm corresponds to $\delta = 0.28(2)$ in $Fe_{3-\delta}O_4$, a value that agrees with the values obtained from the Mössbauer spectral analysis proposed below.

MÖSSBAUER SPECTROSCOPY

The iron-57 Mössbauer spectra measured at 300 K for the nanorings, short-nanotubes, and long-nanotubes, also designated as α-Fe_2O_3/Fe_3O_4/γ-Fe_2O_3, are shown in Figure 4a−c of the paper by Niraula et al.[1] These spectra should prove very useful in confirming the Rietveld refinements and delineating the composition and magnetic properties of the nanoparticles under study. Unfortunately, serious misfits are clearly visible for the nanoring spectrum at ca. −8 and +8.5 mm/s and similarly for the short- and long-nanotubes spectra.

Further, as indicated in Table S4 by Niraula et al.,[1] the population of Fe^{3+} on the A sites of Fe_3O_4 is about 3−4 times, instead of the stoichiometric 0.5, the population of $Fe^{2.5+}$ on the

https://doi.org/10.1021/acsanm.2c03571
ACS Appl. Nano Mater. 2022, 5, 14031−14037

B sites. Niraula et al.[1] justify this discrepancy by "the presence of a large number of cation vacancies and the defective region on the B-sites". This justification is not valid because the presence of vacancies on the B sites of Fe_3O_4 must be charge-balanced by the presence of Fe^{3+} on the B sites, as is explained in detail below. Hence, the composition of Fe_3O_4 with Fe^{3+} on the A sites and only $Fe^{2.5+}$ on the B sites of $Fe_{3-\delta}O_4$, as given in Table S4,[1] is incorrect.

The above problems present in the analysis[1] of the three Mössbauer spectra have prompted us to undertake a further detailed analysis of these spectra.

Because it seems that Niraula et al.[1] are either unable or unwilling to make available the original Mössbauer spectral data, we have digitized their three published spectra and present herein their detailed spectral analysis. The failure earlier[1] to include the scale of the percent transmission associated with each spectrum has made the digitization process somewhat complex.[8] A maximum absorption of 5% and a baseline count of $n \sim 500000$, which gives a statistical uncertainty of $100/n^{1/2}$, were assumed for the digitization and fitting processes; see the Supporting Information for additional details concerning the digitization. In spite of these assumptions, the result of the digitization process seems to be successful, as is shown in Figure 2 by the black plus signs.

During the initial fits of the digitized Mössbauer spectra, it soon became clear that the published fits shown in Figure 4a−c[1] are far from the best fits of the spectral data. Major spectral misfits are obvious in the residuals associated with the parameters reported by Niraula et al.,[1] as is shown at the top of Figure S1, which used the reported parameters in their Table S4.[1] In reality, as far as we can determine, the fits of the three Mössbauer spectra shown in Figure 4a−c[1] are most probably simulations of the spectra obtained by using bulklike hyperfine parameters corresponding to a fixed isomer shift, I.S., quadrupole shift, Q.S., hyperfine field, B_{hf}, and relative spectral area or population %, with the population being adjusted to agree somewhat with the X-ray structural results. In addition, it is not clear what "standard parameters[45] of γ-Fe_2O_3" were used by Niraula et al.[1] in their fits because only parameters for Fe_3O_4 are given in their ref 45.

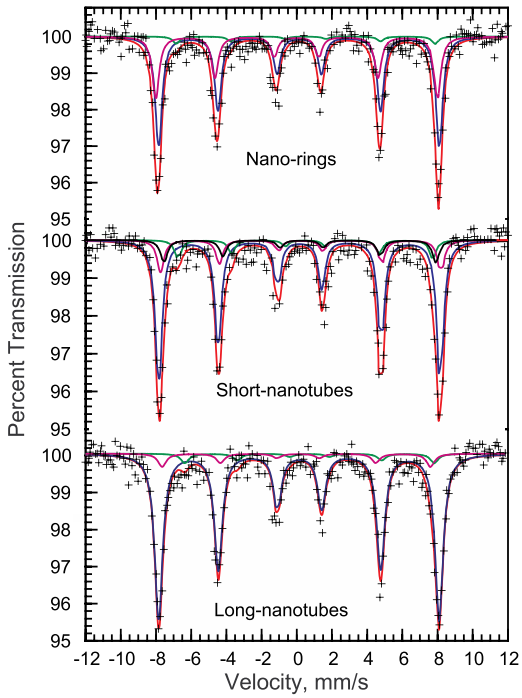

Figure 2. Mössbauer spectra obtained at 300 K for the nanorings and short- and long-nanotubes. The red solid lines show the best fit with the minimum number of sextets. The green, purple, and blue solid lines are assigned to the valence-averaged $Fe^{2.5+}$ cations on the B sites and Fe^{3+} on the A and B sites of the solid solutions $^{A}Fe^{3+}[^{B}Fe_{2(1-3\delta)}{}^{2.5+}Fe_{5\delta}{}^{3+}\square_{\delta}]O_4$. The black solid line is assigned to α-Fe_2O_3 in the spectrum of the short-nanotubes. The residuals for each fit are shown in Figure S2. In the long-nanotubes spectrum the red line best fit is almost obscured by the blue line of the Fe^{3+} B/A site.

At this point, it should be noted that, herein, all of the spectral components in a given Mössbauer spectrum have been fit with the same full-width at half-maximum, Γ; for some unknown reason and in spite of having been suggested by Nayak,[4] no spectral line widths are given in the Niraula et al.[1,S] papers. Our experience indicates that the quality of the reported Mössbauer spectral data[1] is insufficient to allow the use of more than one line width in a given spectral fit, a single line width that may or may not have been used in ref 1. Herein, the best-fit line widths range from 0.47(2) mm/s for both the nanorings and short-nanotubes to 0.558(6) mm/s for the long-nanotubes; see Tables 1 and S1−S4, which report all of the Mössbauer spectral parameters obtained for the spectral fits shown in Figures 2 and S1 and S2.

In the study of the digitized Mössbauer spectra, it soon became apparent that the published spectra in Figure 4a−c[1] are plotted relative to the rhodium matrix source; in Tables 1 and S1−S4, the isomer shifts, δ_{Fe}, have been converted to the more usual values reported[9] relative to 295 K α-iron by adding 0.12 mm/s to each isomer shift. Further, as pointed out by Nayak,[4] it has been found that any attempt to independently fit the A and B iron(III) sites in maghemite, γ-Fe_2O_3, leads either to virtually perfect correlation coefficients between varied parameters or to very poor, often physically unreasonable fits. Hence, the fits shown in Figure 2 have been obtained with the minimum number of sextets that give a statistically acceptable χ^2 in view of the two above assumptions; the resulting spectral parameters are given in Table 1 for the analysis in terms of solid solutions of Fe_3O_4 and γ-Fe_2O_3 described below and in Table S1 for the assignment used earlier.[1]

MÖSSBAUER SPECTRAL ANALYSIS IN TERMS OF SOLID SOLUTIONS OF Fe_3O_4 AND γ-Fe_2O_3

In view of the very large spectral line widths noted above and both the criticism of Nayak[4] and the excellent analyses by Gorski and Scherer,[10] it seems quite unreasonable to us to divide the Mössbauer spectral analysis into sextets assigned to the A and B sites of both magnetite and maghemite, Fe_3O_4 and γ-Fe_2O_3, respectively.

The assignment of the sextets follows the expected stoichiometry[10] for uniform solid solutions of Fe_3O_4 and γ-Fe_2O_3, i.e., $^{A}Fe^{3+}[^{B}Fe_{1-3\delta}{}^{2+}Fe_{1+2\delta}{}^{3+}\square_{\delta}]O_4$, where $\square$ represents a vacancy, $\delta = 0$ corresponds to Fe_3O_4, and $\delta = 0.333$ corresponds to γ-Fe_2O_3. This stoichiometry clearly shows that the presence of δ vacancies on the B sites is charge-balanced by an increase of 2δ Fe^{3+} cations and a decrease of 3δ Fe^{2+} cations on the B sites, relative to the Fe^{3+} and Fe^{2+} populations of one in perfectly stoichiometric Fe_3O_4. At 300 K, well above the nominal 121 K temperature of the Verwey transition of magnetite, the Fe^{2+} and Fe^{3+} cations on the B sites are valence-averaged and observed as $Fe^{2.5+}$ cations in the

https://doi.org/10.1021/acsanm.2c03571
ACS Appl. Nano Mater. 2022, 5, 14031−14037

Table 1. Mössbauer Spectral Analysis in Terms of Uniform Solid Solutions of Fe_3O_4 and γ-Fe_2O_3[a]

sample	cation	site	Γ, mm/s	δ_{Fe},[b] mm/s	H, T	area, %	χ^2[c]
nanorings	Fe^{3+}	B	0.47(2)	0.255	49.5	62(6)	2.737
	$Fe^{2.5+}$	B	0.47(2)	0.624	45.6	4(1)	
	Fe^{3+}	A	0.47(2)	0.11(2)	49.69(7)	34(5)	
short-nanotubes	Fe^{3+}	B/A	0.47(2)	0.28	49.6(1)	66(13)	2.053
	$Fe^{2.5+}$	B	0.47(2)	0.61	44.9(3)	8(1)	
	Fe^{3+}	A	0.47(2)	0.34	49.4(5)	15(6)	
	α-Fe_2O_3		0.47(2)	0.35	47.9(4)	10(5)	
long-nanotubes	Fe^{3+}	B/A	0.558(6)	0.262(3)	49.46(2)	88(2)	2.125
	$Fe^{2.5+}$	B	0.558(6)	0.85(5)	44.0(4)	5.0(7)	
	Fe^{3+}	A	0.558(6)	0.15(4)	47.3(3)	7(1)	

[a]The assignment is based on the solid solutions stoichiometry $^{A}Fe^{3+}[^{B}Fe_{2(1-3\delta)}{}^{2.5+}Fe_{5\delta}{}^{3+}\square_{\delta}]O_4$. The quadrupole shift values, all of which are essentially zero, have been omitted. The statistical uncertainties for the fitted parameters are given in parentheses. There is no significant correlation between any of the parameters listed. [b]The isomer shifts, δ_{Fe}, are given relative to α-iron foil at 295 K. [c]In the absence of the actual counts in the spectra, the χ^2 values have been estimated from the statistical uncertainty, as explained in the text.

Mössbauer spectra of Fe_3O_4 or solid solutions of Fe_3O_4 and γ-Fe_2O_3. Hence, the stoichiometry of solid solutions of Fe_3O_4 and γ-Fe_2O_3 observed by Mössbauer spectroscopy is $^{A}Fe^{3+}[^{B}Fe_{2(1-3\delta)}{}^{2.5+}Fe_{5\delta}{}^{3+}\square_{\delta}]O_4$.

The only clearly identifiable component in the Mössbauer spectra shown in Figure 2 is the green sextet with the largest isomer shift, δ_{Fe}, of 0.6−0.8 mm/s, a sextet that is assigned (Table 1) to the B-site valence-averaged $Fe^{2.5+}$ cations. For the nanorings, its percent area is 4(1)%, and thus its relative spectral area is

$$0.04(1) = \frac{2(1-3\delta)}{3-\delta}$$

or δ = 0.315(5), which corresponds to the stoichiometry $^{A}Fe^{3+}[^{B}Fe_{0.11(3)}{}^{2.5+}Fe_{1.575(25)}{}^{3+}\square_{0.315(5)}]O_4$. Hence, the expected Fe^{3+} A- and B-site relative areas are 0.3724(7) and 0.587(11), in reasonable agreement with the observed values of 0.34(5) and 0.62(6).

For the long-nanotubes, the relative spectral area of 0.050(7) for the B-site $Fe^{2.5+}$ component leads to a stoichiometry of $^{A}Fe^{3+}[^{B}Fe_{0.14(3)}{}^{2.5+}Fe_{1.550(25)}{}^{3+}\square_{0.310(5)}]O_4$ and, hence, to the expected Fe^{3+} A- and B-site relative areas of 0.3717(7) and 0.576(10), in apparent disagreement with the observed values of 0.07(1) and 0.88(2); see the percent areas of 7(1) and 88(2)% in Table 1. However, the broad line width of 0.558(6) mm/s indicates that the Fe^{3+} A and B cations experience a distribution of the environment, and thus some of the Fe^{3+} A site cations are included in the most intense sextet.

Finally, for the short-nanotubes, the presence of α-Fe_2O_3 complicates the calculation a bit, but the relative spectral area of 0.09(1) for the B-site $Fe^{2.5+}$ component leads to a stoichiometry of $^{A}Fe^{3+}[^{B}Fe_{0.242(24)}{}^{2.5+}Fe_{1.465(20)}{}^{3+}\square_{0.293(4)}]O_4$ and, hence, to the expected Fe^{3+} A- and B-site relative areas of 0.3694(5) and 0.541(8), in apparent disagreement with the observed values of 0.17(7) and 0.73(14), obtained after correction for 10% of hematite, α-Fe_2O_3, from the percent areas of 15(6) and 66(13)% (Table 1). The short-nanotube spectrum is of poorer quality than those for the nanorings and long-nanotubes, as shown by the statistical noise in Figure 2. Hence, our attempt to fit the isomer shifts, δ_{Fe}, given in Table 1 was unsuccessful, and the isomer shifts were fixed to the values reported by Niraula et al.[1] It is not impossible that a more reasonable fit of this spectrum could be obtained with spectral parameters that are more similar to those observed for the nanorings and long-nanotubes.

In all three cases, the number of B-site vacancies, i.e., δ = 0.315(5), 0.293(4), and 0.310(5) for the nanorings and short- and long-nanotubes, respectively, is close to δ = 0.333 for γ-Fe_2O_3 and in agreement with δ = 0.28(2) obtained from the average lattice parameter of 0.8355(10) nm; hence, these nanoparticles are very rich in γ-Fe_2O_3. We believe that the analysis of both the X-ray diffraction and Mössbauer spectral results in terms of the expected stoichiometry for solid solutions of Fe_3O_4 and γ-Fe_2O_3, i.e., $^{A}Fe^{3+}[^{B}Fe_{1-3\delta}{}^{2+}Fe_{1+2\delta}{}^{3+}\square_{\delta}]O_4$, is more reasonable and experimentally better supported than an analysis[1] in terms of nonstoichiometric separate grains of Fe_3O_4 and γ-Fe_2O_3.

MATHEMATICAL EQUATION PROBLEMS

Several equations found in the original text of the paper by Niraula et al.[1] are either wrong or incomplete, all of which simply adds confusion to the paper. In some but not all of these cases it seems the corresponding computations are, at least, close to correct, but in some other cases, either the computations are incorrect or insufficient information is included in the paper to permit a check of their validity.

In the following discussion, we have used the same equation numbers as those used earlier[1] and have added primes to related new equations.

The second, unnumbered, portion of the formula found[1] in the left column of page 3150 is wrong, as clearly indicated by a unit analysis. The correct equations[11] are

$$\mathrm{SAR} = \left(\frac{CM}{m_{\mathrm{MNP}}}\right)\left(\frac{\mathrm{d}T}{\mathrm{d}t}\right)$$

and

$$\mathrm{ILP} = \frac{\mathrm{SAR}}{fH^2} = \left(\frac{CM}{m_{\mathrm{MNP}}fH^2}\right)\left(\frac{\mathrm{d}T}{\mathrm{d}t}\right)$$

where SAR is the specific heat absorption rate (W/kg), C is the specific heat capacity of the fluid medium, predominately water [J/(kg K)], M is the mass of the fluid, m_{MNP} is the mass of the nanoparticles, $\mathrm{d}T/\mathrm{d}t$ is the initial slope of heating, f is the frequency (Hz or s^{-1}), and H is the applied magnetic field (A/m). ILP, the intrinsic loss of power, thus has the SI units of H m^2 kg^{-1}, as correctly indicated in the right column of page 3154, and it seems that the correct equation has been used by Niraula et al.[1]

https://doi.org/10.1021/acsanm.2c03571
ACS Appl. Nano Mater. 2022, 5, 14031−14037

Unfortunately, it is not clear how Niraula et al.[1] determined the initial dT/dt from the somewhat nonlinear behavior of heating with time from their Figures S9a−c and S10f. Indeed, Wildeboer et al.[11] have studied in detail how different methods used in determining the initial dT/dt affect the value of the specific heat absorption rate and described the best procedure to obtain the most accurate SAR values. In the absence of a description of the procedure used by Niraula et al.[1] to obtain dT/dt and the specific heat absorption rate, no uncertainty and possibly no confidence can be placed in the reported values. Further, for some unknown and never-mentioned reason, there are seemingly unexpected,[1] nontrivial, decreases in temperature after ca. 300 s in several of the heating profiles shown in Figures S9 and S10. One possible reason for these decreases may be evaporative cooling, as pointed out by Wildeboer et al.[11]

Equation 2

$$K_S = \left(\pi - \frac{3}{4}N_C\right)M_S^2 \tag{2}$$

yields K_S, the shape anisotropy constant, for a shape-defined demagnetizing factor, N_C. Unfortunately, the meaning of eq 3 is undefined[1] in the left column of page 3154

$$\left[\frac{\rho}{\sqrt{\rho^2 - 1}}\ln(\rho + \sqrt{\rho^2 - 1}) - 1\right] \tag{3}$$

and is also wrong for the definition of the unitless shape demagnetizing factor,[12] N_C, which should read

$$N_C = \frac{4\pi}{\rho^2 - 1}\left[\frac{\rho}{\sqrt{\rho^2 - 1}}\ln(\rho + \sqrt{\rho^2 - 1}) - 1\right] \tag{3'}$$

where ρ is c/a, the ratio of the major axis or length, c, to the minor axis or outer diameter, a, of the nanoparticles.

By using eqs 2 and 3′, Vallejo-Fernandez and O'Grady[12] have calculated and plotted in their Figure 3, the dependence of the shape anisotropy constant, K_S, of magnetite nanoparticles, with M_S = 480 emu/cm^3 as a function of ρ. The reader should note that K_S increases from zero for ρ = 1 to 6.5 × 10^5 erg/cm^3 for ρ = 14, i.e., values that are approximately 100 times the K_S values quoted three lines below eq 3 in ref 1. Herein, Figure S3 shows the ρ dependence of the shape anisotropy constant, K_S, of the nanoparticles studied by Niraula et al.,[1] with M_S = 84 emu/g, or for the 5.24 g/cm^3 density of magnetite, M_S = 440 emu/cm^3. We recalculated the values of ρ from the mean and Gaussian size distribution values given in Figure 2 in ref 1 and obtained ρ = 1.37(0.63), 1.64(0.67), and 2.25(0.84) for the nanorings and short- and long-nanotubes, respectively. These values are within their uncertainties. close but not identical to those given for $\beta = \rho$ on page 3155, left column, five lines from the bottom.[1] We obtain 1.37 ≤ ρ < 2.00, M_S = 88 emu/g, and 1.45 × 10^5 ≤ K_S < 2.92 × 10^5 erg/cm^3 for the nanorings, 1.64 ≤ ρ < 2.31, M_S = 84 emu/g, and 2.40 × 10^5 ≤ K_S < 3.71 × 10^5 erg/cm^3 for the short-nanotubes, and ρ = 2.25 (0.84), M_S = 84 emu/g, and 1.70 × 10^5 ≤ K_S < 4.20 × 10^5 erg/cm^3 for the long-nanotubes. These values are similar to those found in ref 12 and are approximately 100 times larger than the values of 2.3 × 10^3, 3.9 × 10^3, and 6.0 × 10^3 erg/cm^3 for the nanorings and short- and long-nanotubes found on page 3154, left column, three lines below eq 3. We could not determine how Niraula et al.[1] arrived at these values, which are also 100 times smaller than the magnetocrystalline anisotropy constant that they quote on page 3149, right column, at the end of section 2.2.6, a value that appears to be correct.

Equation 4 found[1] on page 3155,

$$A = 3.53\mu_0 M_S H_{max}(1 - 0.7\kappa) \tag{4}$$

gives the area, A, of the hysteresis loop and thus the energy density that can be provided by the hysteresis loop to heat a cell. The authors note that "... κ is a nondimensional [sic] constant that is negligible for ferrimagnetic materials". This statement is not supported by the literature. Indeed, the non-dimensional parameter, κ, has been introduced by Usov and Grebenshchikov[13] to account for the dependence of the coercive field, H_C, on the frequency, f, of the applied alternating-current (ac) field, H,

$$\mu_0 H_C = \mu_0 H_K(1 - \kappa^{1/2})$$

where H_K is the anisotropy field and κ is given by

$$\kappa = \frac{k_B T}{K_A V}\ln\left(\frac{k_B T}{4\mu_0 M_S V H f \tau_0}\right)$$

where k_B is the Boltzmann constant, T is the temperature, K_A is the anisotropy constant, V is the volume of the particle, μ_0 is the permeability of a vacuum, M_S is the saturation magnetization, H is the strength of the applied ac field at a frequency f, and τ_0 is the frequency factor of the Néel−Brown relaxation time[14,15] taken equal to 10^{-10} s. We estimated κ = 6 × 10^{-6} for the nanorings for an applied ac field of 200 Oe, and it is indeed negligible but not for the reason indicated above, i.e., "... negligible for ferrimagnetic materials". The reader should note that the *frequency* dependence of the coercive field has not been studied by Niraula et al.[1]

Carrey et al.[16] elaborated on the dependence of the coercive field, H_C, on the frequency, f, of the applied ac field, H, and wrote

$$\mu_0 H_C = 0.48\mu_0 H_K(1 - \kappa^{0.8})$$

Thus, the area of the hysteresis loop is given by

$$A = 1.92\mu_0 M_S H_K(1 - \kappa^{0.8}) \tag{4'}$$

The phenomenological eq 4′ appears[16] to be valid for κ < 0.5.

By building upon the work of Carrey et al.,[16] Tong et al.[17] wrote another phenomenological equation, eq 4 given on page 3155 and used by Niraula et al.[1] Note that, in eq 4, the anisotropy field, H_K, has been replaced by the strength of the applied ac field, a rather surprising replacement. Equation 4 applies[17] to nanoparticles of 33 and 40 nm, i.e., one order of magnitude smaller than those studied by Niraula et al.[1] Hence, there is no assurance whether or not the phenomenological eq 4 may be valid for the larger particles of ca. 300 nm. However, Niraula et al.[1] built further upon the Tong et al.[17] model by using their eq 5 on page 3155,[1]

$$A = 3.53\mu_0 M_S H_{max}(1 - 0.7\kappa)\beta \tag{5}$$

where $\beta = \rho$ in the above eq 3′. We do not see any justification for multiplying the area of the hysteresis loop by $\beta = \rho$, the unitless anisotropy shape factor; at least it is *unitless* and does not raise any unit problems. Note that the use of μ_0 in eq 5 implies the use of SI units in this equation.

If eq 5 with κ = 0 is used to obtain the area in J/m^3 of the hysteresis loop plotted as M in A/m versus H in A/m, eq 6′ *must* be used[18] to obtain SAR in W/kg,

$$SAR = fA/d \tag{6'}$$

https://doi.org/10.1021/acsanm.2c03571
ACS Appl. Nano Mater. 2022, 5, 14031−14037

where d is the density (kg/m^3) of the nanoparticles. Equation 6, as given on page 3155, applies[19] only if the area of the hysteresis loop is obtained from a plot of the reduced magnetization, M/M_S, versus H, and thus eq 6 is incompatible with the simultaneous use of eqs 4 and 5.

In conclusion, it is impossible to check the SAR values plotted in Figure 6 because eqs 5 and 6 apply to hysteresis curves plotted in different forms and possibly written with different unit systems. Further, the saturation magnetizations measured in the applied ac fields are *not* reported and the density used in the calculation is *not* specified. Finally, the comparison with the experimental values is equally difficult because the authors do not explain how they obtained the dT/dt slope.

CONCLUSIONS

Scanning electron microscopy reveals that, when the size distributions derived from the Gaussian distribution of the particle lengths and outer diameters, D_{out}, all in nm, for the nanoparticles are taken into consideration, there is relatively little difference between the short-nanotubes and long-nanotubes lengths and outer diameters. Further, the nanoparticle lengths range from 275 ± 51 to 515 ± 98 nm and their outer diameters range from 201 ± 55 to 251 ± 46 nm, indicating that the dimensions of the nanoparticles under study are far larger than those of typical nanoparticles.[22]

From the reformulation of the stoichiometry of all three nanoparticles under study herein in terms of solid solutions of Fe_3O_4 and γ-Fe_2O_3, $^{A}Fe^{3+}[^{B}Fe_{1-3\delta}{}^{2+}Fe_{1+2\delta}{}^{3+}\square_{\delta}]O_4$, the number of B-site vacancies, i.e., $\delta = 0.315(5)$, $0.293(4)$, and $0.310(5)$, for the nanorings, short-nanotubes, and long-nanotubes, respectively, is close to $\delta = 0.333$ for γ-Fe_2O_3, and in agreement with $\delta = 0.28(2)$ obtained from the average lattice parameter of 0.8355(10) nm, for all three nanoparticles. Thus, these particles are very rich in γ-Fe_2O_3 and not in Fe_3O_4. We believe that the analysis of both the X-ray diffraction and Mössbauer spectral results in terms of the expected stoichiometry for the solid solutions of Fe_3O_4 and γ-Fe_2O_3 studied above the Verwey transition, i.e., $^{A}Fe^{3+}[^{B}Fe_{2(1-3\delta)}{}^{2.5+}Fe_{5\delta}{}^{3+}\square_{\delta}]O_4$. is more reasonable and experimentally better supported than an analysis[1] in terms of nonstoichiometric separate grains of Fe_3O_4 and γ-Fe_2O_3.

The analysis and, in some cases, the resolution reported herein, of the errors in the mathematical equations and their use indicate that the reader must exercise extreme caution in using the published expressions and many of the derived results found in the paper published by Niraula et al.[1] Although the "Comment" published[4] by Nayak is correct, it reported only a few of the existing problems found in Niraula et al.[1] Further, the "Reply" published[5] by Niraula and Sharma completely ignored the valuable comments of Nayak.[4] Sadly, many of the errors and related difficulties noted above also may be found in two previous papers[20,21] published by many of the same authors as the Niraula et al.[1] paper.

Recently, Winsett et al.[22] have reported on the quantitative determination of the amount of magnetite, Fe_3O_4, and maghemite, γ-Fe_2O_3, by Mössbauer spectroscopy in highly crystalline nanoparticles with a size distribution of 7 ± 2 nm that have been prepared by the exposure of magnetite to dioxygen with a consequent partial conversion of some of the Fe^{2+} or $Fe^{2.5+}$ found in magnetite to Fe^{3+}, thus forming maghemite, γ-Fe_2O_3. Their resulting powder X-ray diffraction results (Figure 1 in ref 22) and their excellent, well-resolved, room temperature Mössbauer spectrum (reported in Figure 5 in ref 22) are very different from those reported in Figure 4 of the Niraula et al.[1] paper. Further, rather surprisingly, in spite of the Mössbauer spectra in the two papers appearing vastly different, the hyperfine parameters reported by Winsett et al.[22] and Niraula et al.[1] are very similar. The reasons for the differences in the two sets of Mössbauer spectra are, at this time, unexpected and perhaps hard to understand, but they likely result from the very different nanoparticle sizes. The nanoparticles in the Winsett et al.[22] sample are magnetic single domain particles of either magnetite or maghemite, whereas the vastly larger Niraula et al.[1] nanoparticles, or more correctly mesoparticles, are magnetic multidomain particles of a solid solution of magnetite and maghemite. These differences in the size, magnetic structure, and composition[1,22] of the nanoparticles most surely result from the very different synthetic methods used in their differing preparations.

At this point, the reader should note that Winsett et al.[22] failed to fit the Mössbauer spectrum with four sextets as proposed by da Costa et al.,[23] who have reported "that if a sample contains both magnetite and maghemite, its Mössbauer spectra should be fitted by four Zeeman sextets ..." where two sextets correspond to the Fe^{3+} A sites of magnetite and maghemite, one sextet corresponds to iron cations of intermediate-valence $Fe^{2.5+}$ in magnetite on the B site, and one sextet corresponds to the Fe^{3+} on the maghemite B site. Winsett et al.[22] report that an "attempt to lock down the parameters to the reported literature[23] values resulted in hyperfine parameters which are not physically acceptable for magnetite and maghemite". This observation provides additional support for the earlier criticism in the comment by Nayak.[4]

ASSOCIATED CONTENT

Supporting Information

The Supporting Information is available free of charge at https://pubs.acs.org/doi/10.1021/acsanm.2c03571.

Digitizing the Mössbauer spectra, Tables S1−S4 (300 K Mössbauer spectral fit parameters for various fitting models), Figures S1 and S2 (fits of the 300 K Mössbauer spectra with different models), and Figure S3 (ρ dependence of the shape anisotropy constant, K_S) (PDF)

AUTHOR INFORMATION

Corresponding Authors

Fernande Grandjean − *Department of Chemistry, Missouri University of Science and Technology, University of Missouri, Rolla, Missouri 65409-0010, United States*; Email: fgrandjean@uliege.be

Gary J. Long − *Department of Chemistry, Missouri University of Science and Technology, University of Missouri, Rolla, Missouri 65409-0010, United States*; orcid.org/0000-0002-6573-5927; Email: glong@mst.edu

Complete contact information is available at: https://pubs.acs.org/10.1021/acsanm.2c03571

Notes

The authors declare no competing financial interest.

REFERENCES

(1) Niraula, G.; Coaquira, J. A. H.; Zoppellaro, G.; Villar, B. M. G.; Garcia, F.; Bakuzis, A. F.; Longo, J. P. F.; Rodrigues, M. C.; Muraca, D.; Ayesh, A. I.; Sinfrônio, F. S. M.; de Menezes, A. S.; Goya, G. F.; Sharma,

https://doi.org/10.1021/acsanm.2c03571
ACS Appl. Nano Mater. 2022, 5, 14031−14037

S. K. Engineering Shape Anisotropy of Fe_3O_4-γ-Fe_2O_3 Hollow Nanoparticles for Magnetic Hyperthermia. *ACS Appl. Nano Mater.* **2021**, *4*, 3148−3158.
(2) The reader should note that the histograms for the lengths and outer diameters of S, SNT, and LNT all exhibit a clearly non-Gaussian distribution.
(3) Grandjean, F.; Long, G. J. Best Practices and Protocols in Mössbauer Spectroscopy. *Chem. Mater.* **2021**, *33*, 3878−3904.
(4) Nayak, P. K. Comment on "Engineering Shape Anisotropy of Fe_3O_4-γ-Fe_2O_3 Hollow Nanoparticles for Magnetic Hyperthermia". *ACS Appl. Nano Mater.* **2022**, *5*, 1715−1716.
(5) Niraula, G.; Sharma, S. K. Reply to Comment on "Engineering Shape Anisotropy of Fe_3O_4-γ-Fe_2O_3 Hollow Nanoparticles for Magnetic Hyperthermia". *ACS Appl. Nano Mater.* **2022**, *5*, 1717−1718.
(6) McCusker, L. B.; Von Dreele, R. B.; Cox, D. E.; Louër, D.; Scardi, P. Rietveld Refinement Guidelines. *J. Appl. Crystallogr.* **1999**, *32*, 36−50.
(7) Cervellino, A.; Frison, R.; Cernuto, G.; Guagliardi, A.; Masciocchi, N. Lattice Parameters and Site Occupancy Factors of Magnetite−Maghemite Core−Shell Nanoparticles. A Critical Study. *J. Appl. Crystallogr.* **2014**, *47*, 1755−1761.
(8) https://apps.automeris.io/wpd/, last accessed on August 8, 2022.
(9) Gütlich, P.; Bill, E.; Trautwein, A. X. *Mössbauer Spectroscopy and Transition Metal Chemistry: Fundamentals and Applications*; Springer-Verlag: Heidelberg, Germany, 2011; p 33, Table 3.1.
(10) Gorski, C. A.; Scherer, M. M. Determination of Nanoparticulate Magnetite Stoichiometry by Mössbauer Spectroscopy, Acidic Dissolution, and Powder X-ray Diffraction: A Critical Review. *Am. Mineral.* **2010**, *95*, 1017−1026.
(11) Wildeboer, R. R.; Southern, P.; Pankhurst, Q. A. On the Reliable Measurements of Specific Absorption Rates and Intrinsic Loss Parameters in Magnetic Hyperthermia Materials. *J. Phys. D: Appl. Phys.* **2014**, *47*, 495003.
(12) Vallejo-Fernandez, G.; O'Grady, K. Effect of the Distribution of Anisotropy Constants on the Hysteresis Loses for Magnetic Hyperthermia Applications. *Appl. Phys. Lett.* **2013**, *103*, 142417.
(13) Usov, N. A.; Grebenshchikov, Y. B. Hysteresis Loops of an Assembly of Superparamagnetic Nanoparticles with Uniaxial Anisotropy. *J. Appl. Phys.* **2009**, *106*, 023917.
(14) Néel, L. Théorie du Trainage Magnétique des Ferromagnétiques en Grains Fins avec Application aux Terres Cuites. *Ann. Géophys.* **1949**, *5*, 99−136.
(15) Brown, W. F., Jr. Thermal Fluctuations of a Single Domain Particle. *Phys. Rev.* **1963**, *130*, 1677−1686.
(16) Carrey, J.; Mehdaoui, B.; Respaud, M. Simple Models for Dynamic Hysteresis Loop Calculations of Magnetic Single-domain Nanoparticles: Application to Magnetic Hyperthermia Optimization. *J. Appl. Phys.* **2011**, *109*, 083921.
(17) Tong, S.; Quinto, C. A.; Zhang, L.; Mohindra, P.; Bao, G. Size-Dependent Heating of Magnetic Iron Oxide Nanoparticles. *ACS Nano* **2017**, *11*, 6808−6816.
(18) Dutz, S.; Hergt, R. Magnetic Nanoparticle Heating and Heat Transfer on a Microscale: Basic Principles, Realities and Physical Limitations of Hyperthermia for Tumour Therapy. *Inter. J. Hyperthermia* **2013**, *29*, 790−800.
(19) Usov, N. A.; Nesmeyanov, M. S.; Tarasov, V. P. Magnetic Vortices as Efficient Nanoheaters in Magnetic Nanoparticle Hyperthermia. *Sci. Rep* **2018**, *8*, 1224−1232.
(20) Niraula, G.; Coaquira, J. A. H.; Aragon, F. H.; Galeano Villar, B. M.; Mello, A.; Garcia, F.; Muraca, D.; Zoppellaro, G.; Vargas, J. M.; Sharma, S. K. Tuning the Shape, Size, Phase Composition and Stoichiometry of Iron Oxide Nanoparticles: The Role of Phosphate Anions. *J. Alloys Compd.* **2021**, *856*, 156940.
(21) Niraula, G.; Coaquira, J. A. H.; Aragon, F. H.; Bakuzis, A. F.; Villar, B. M. G.; Garcia, F.; Muraca, D.; Zoppellaro, G.; Ayesh, A. I.; Sharma, S. K. Stoichiometry and Orientation- and Shape-Mediated Switching Field Enhancement of the Heating Properties of Fe_3O_4 Circular Nanodiscs. *Phys. Rev. Applied* **2021**, *15*, 014056.
(22) Winsett, J.; Moilanen, A.; Paudel, K.; Kamali, S.; Ding, K.; Cribb, W.; Seifu, D.; Neupane, S. Quantitative Determination of Magnetite and Maghemite in Iron Oxide Nanoparticles Using Mössbauer Spectroscopy. *SN Appl. Sci.* **2019**, *1*, 1636.
(23) da Costa, G. M.; De Grave, E.; Vandenberghe, R. E. Mössbauer Studies of Magnetite and Al-substituted Maghemites. *Hyperfine Interact.* **1998**, *117*, 207−243.

https://doi.org/10.1021/acsanm.2c03571
ACS Appl. Nano Mater. 2022, 5, 14031−14037